

## Original Article

# Estimation of the risk of secondary malignancies following intraoral electron radiotherapy for tongue cancer patients

Seonghoon Jeong<sup>1</sup>, Myonggeun Yoon<sup>1</sup>, Weon Kuu Chung<sup>2</sup>†, Mijoo Chung<sup>2</sup>, Dong Wook Kim<sup>2</sup>

<sup>1</sup>*Department of Bio-Convergence Engineering, Korea University, <sup>2</sup>Department of Radiation Oncology, Kyung Hee University Hospital at Gangdong, Seoul, Korea*

(Received 21 April 2016; revised 21 September 2016; accepted 21 September 2016; first published online 28 November 2016)

## Abstract

**Purpose:** To measure dosimetric characteristics for linear accelerator-based electron beams, which are applied through locally manufactured acrylic tubes for intraoral radiotherapy and to calculate the secondary cancer risk for organs at risk.

**Materials and methods:** Six different acrylic tubes were exposed to a 6-MeV electron beam; they had tips with three angles (0°, 15° and 30°) and two diameters (2.5 and 3.0 cm). Gafchromic EBT2 film was horizontally and vertically inserted in a solid water phantom to measure the dose profiles and percentage depth doses (PDDs). The measured data from radio-photoluminescence glass dosimeters placed on the neck and both eyes were used to estimate the lifetime attributable risk of secondary cancer resulting from intraoral radiotherapy for tongue cancer.

**Results:** A total of 12 dose profiles were obtained from six different acrylic applicators at 0.5 and 1.28 cm depths. Circular shapes were obtained from 0° applicators, and oval shapes were obtained from 15° and 30° applicators. Absorbed doses at a 0.5 cm depth were higher than those at a 1.28 cm depth. PDD shapes for the six acrylic applicators were similar to those of a normal 6 MeV electron beam. Larger-diameter applicators showed higher PDD than smaller-diameter applicators with the same tip angle. According to our secondary cancer risk estimation, if 100,000 patients received intraoral radiotherapy at 30 years and lived until 80 years, 122 female and 22 male patients would develop secondary thyroid cancer, while 13 female and 18 male patients would develop secondary ocular melanoma or retinoblastoma.

**Conclusions:** Dosimetric characteristics for linear accelerator-based intraoperative radiotherapy treatment beam were confirmed. In addition, we found that 0.1% of tongue cancer patients would get secondary malignancies for both eyes and thyroid from this treatment.

**Keywords:** dose; electron radiotherapy; intraoral cone radiotherapy; radio-photoluminescence glass dosimeter; secondary cancer risk

† Weon Kuu Chung and Dong Wook Kim equally contributed as corresponding authors.

Correspondence to: Weon Kuu Chung, Department of Radiation Oncology, Kyung Hee University Hospital at Gangdong, Dongnam-ro 892, Gangdong-Gu, Seoul 134-727, Korea. Tel: +82 2 440 7398. Fax: +82 2 440 7393. E-mail: wkchung@khnmc.or.kr, joocheck@gmail.com

## INTRODUCTION

In the early 1960s, Abe and Takahashi<sup>1</sup> of Tokyo University began studying intraoperative radiotherapy (IORT). IORT is a treatment method that exposes a tumour to direct radiation during surgery.<sup>2,3</sup> Some reports have claimed that IORT with external beam irradiation can improve survival in patients with localised tumours.<sup>4–6</sup> The electron beam is characterised by rapid dose fall off such that it irradiates the cancerous area on the surface region intensively, while deeper placed normal tissues are more protected.<sup>7–10</sup> This treatment method uses an electron-guiding device to irradiate treatment target doses precisely in both intraoperative and postoperative radiotherapy of the intraoral cavity. The electron-guiding device is usually cylindrical in shape with a variably angled tip. Different devices have different diameters and tip angles, so the size of the treatment beam can be adjusted to the tumour size.<sup>11–13</sup> The report of the American Association of Physicists in Medicine Task Group 72<sup>14</sup> provides medical physicists with information relating to appropriate room selection, radiation shielding, and equipment for IORT, as well as the required acceptance test and guidelines for clinical operation. Piriz et al.<sup>15</sup> used five different applicators with varying tip angles to administer 6, 9 and 12 MeV electron beams to determine their percentage depth dose (PDD) and isodose curves. They found that a small cone contributes to uniform isodose distribution and homogeneity of radiation dose and that 50% of isodose curves have a diameter close to that of the applicator. They also showed that the measured R<sub>50</sub>, which is the depth, where 50% of the maximum dose occurs for each applicator depends on the electron beam energy and on the angle and radius of the acrylic applicator.

In our study, a patient with a malignant neoplasm of the tongue and lateral floor of the mouth (alveolar ridge) with mandibular invasion (T4N1) was treated with oral-cavity IORT using a 6 MeV electron beam. Using a water-equivalent solid phantom, we assessed the characteristics of the 6 MeV electron beam by measuring the PDD, profile, and output factors. During each of ten 300 cGy treatment sessions, radio-photoluminescence glass dosimeters

(RPLGDs; GD-302M; Asahi Techno Glass Co., Tokyo, Japan) were placed on the patient's neck and both eyes and used to measure the radiation scattered from the treatment site; dosimeter data were then used to estimate secondary cancer risks associated with IORT for the thyroid and both eyes (such as ocular melanoma or retinoblastoma).

## MATERIALS AND METHODS

### Measurement setup

Before treating the patient, we forecast the behaviour of the electron beam in the patient's body using a treatment-planning system, using computed tomography images of a tongue cancer patient as reference (Brilliance CT Big Bore Oncology, Philips Medical Systems, Eindhoven, the Netherlands). Dose distribution in the patient's body was predicted using Eclipse (Varian Medical Systems, Palo Alto, CA, USA). After evaluation of planning, treatment was performed.

The cancer patient was exposed to a 6 MeV electron beam that was focussed upon the target volume through an acrylic cylinder 2.5 cm in diameter and 0.2 cm in thickness with a 30° angle. The acrylic cylinder was attached to an electron beam applicator that could be removed from its gantry (21iX Linear Accelerator; Varian Medical Systems). The tip of the acrylic cylinder was inserted into the patient's mouth, and the electron beam was passed through the acrylic cylinder. Electron beams were projected in a 6 × 6 cm field with an IORT cone and a source-surface distance (SSD) of 100 cm. In IORT, the SSD is defined as the distance from the source to the centre of the slope surface. The sloped applicator was in contact with the surface of the patient's tongue (see Figure 1).

### Calibration of the RPLGDs

In this study, we used RPLGDs (0.15 cm in diameter, 0.85 cm in length) to measure the absorbed dose of radiation below the patient's tongue and organs at risk (OARs; thyroid and eyes including lens, retina, choroid, etc. in this study) to estimate the total dose absorbed by the target. RPLGDs were used because they are easy to use for in vivo measurement. When the irradiated

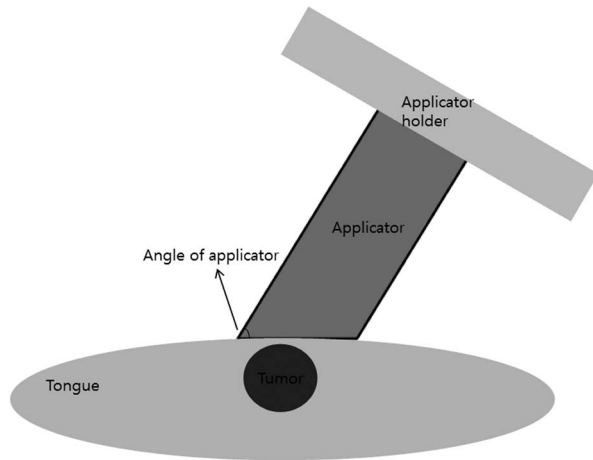


Figure 1. Diagram of intraoperative radiotherapy treatment using acrylic applicator.

dosimeters were exposed to 365 nm ultraviolet light, they emitted orange light (500–700 nm); the stronger the intensity, the greater the absorbed dose of radiation. RPLGD measurements have good reproducibility, and RPLGDs have low energy dependency at high energy (>200 keV), low angular dependency, and low toxicity in the human body.<sup>16–21</sup>

To calibrate the RPLGD, a 6 MeV electron beam was focussed upon a 10 × 10 cm open field. Electron beams of 10, 25, 50, 75, 100, 200 and 300 MU were applied to RPLGDs at 1.28 cm depth of the solid water phantom and 100 cm of SSD.

**Calibration of the EBT2 film**

Gafchromic EBT2 film (International Specialty Products, Alps Road, Wayne, NJ, USA) was also used to measure the behaviour of the electron beam in a water-equivalent phantom. Gafchromic EBT2 film has a wide dosage range (1 cGy to 40 Gy), energy-independent dose response, low radiation scatter and high spatial resolution.<sup>22,23</sup>

To estimate the dose response of Gafchromic EBT2 film, 10 × 10 cm open-field electron beams of 0, 5, 10, 20, 40, 60, 80, 100, 130, 160, 200, 250 and 300 MU were applied to EBT2 film at a beam-centre depth of 1.28 cm. Nine hours after the EBT2 film was exposed to the electron beam, it would stabilise, and a scan would be

carried out using a film scanner (EPSON Expression 1680 Pro; Epson Co., Shinjuku, Japan).

**Measurement of electron beam output**

To measure the behaviour of the electron beam in water and a water-equivalent phantom, we prepared six different acrylic cylinders with diameters of 2.5 and 3.0 cm, 0.2 cm thickness, and 0°, 15° and 30° angles. By contacting the surface of the PPC40 chamber (IBA Dosimetry, Schwarzenbruck, Germany) to the Blue Phantom 2 water phantom (IBA Dosimetry), the electron beam output was measured. The PDD and beam profile were measured using the solid water-equivalent phantom with contact between the tips of the acrylic cylinders and the phantom. Gafchromic EBT2 film was used for this measurement.

**Secondary cancer risk evaluation**

Estimations of secondary cancer risk were also performed. RPLGDs were placed on the patient’s neck and eyebrows to estimate the secondary cancer risk for the thyroid and both eyes. Cancer at eyes could be ocular melanoma, retinoblastoma, etc. Data acquisitions from neck and eyebrows could be replaced with secondary doses at thyroid and both eyes. Secondary doses for both eyes were measured individually because it could be different from each other for a reason such as patient setup error. Data were acquired ten times during intraoperative radiotherapy with the RPLGDs in the same position each time. The excess absolute risk (EAR index) was calculated, originally derived by Schneider et al.<sup>24</sup> from statistical data on atomic bomb survivors and medical patients:

$$EAR (D, s, e, a) = \beta \cdot OED \cdot \exp \left( \gamma_e \cdot (e - 37) + \gamma_a \cdot \ln \left( \frac{a}{46} \right) \right) (1 \pm s)$$

where + is for female, – for male,  $\beta$  the initial slope, OED the organ effective dose,  $s$  related to gender,  $e$  the age at exposure, and  $a$  the age attained. Plateau models using three kinds of OED calculation methods were used for this experiment.<sup>25</sup>

The plateau dose-response model is

$$OED = \frac{1}{V} \sum_i V_i \left( \frac{1 - \exp(-\sigma D_i)}{\sigma} \right)$$

where  $V$  is the organ volume and  $D$  the dose. The parameter  $\sigma$  is used to determine the dose-response for each organ.

Finally, the lifetime attributable risk (LAR)—the number of people who would develop secondary cancer in the organ out of every 100,000 people exposed to radiation—could be

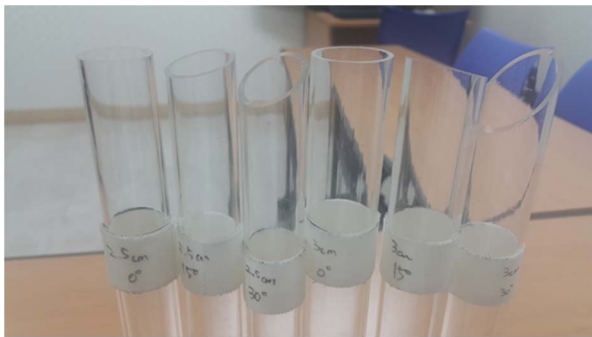


Figure 2. Photograph of acrylic applicator.

calculated from EAR and OED by the following equation:

$$LAR = EAR \cdot \frac{S(a)}{S(e)} \cdot (a - e)$$

**RESULTS**

**PDD**

The PDDs for the six different electron beams of 500 MU with different diameters (2.5, 3 cm) and three angles (0°, 15°, 30°) were measured in the solid water-equivalent phantom on Gafchromic EBT2 film. The photograph of six applicators is represented in Figure 2. Figure 3 show the PDD profiles of six cylinders. Cylinders 3 cm in diameter exposed the solid water phantom to higher radiation doses than did cylinders 2.5 cm in diameter. Slight changes in the radiation dose patterns were observed when cylinders with different slope angles were attached.

**Dose profile**

Dose profiles were measured for each electron beam, with an SSD of 100 cm, at depths of 0.5

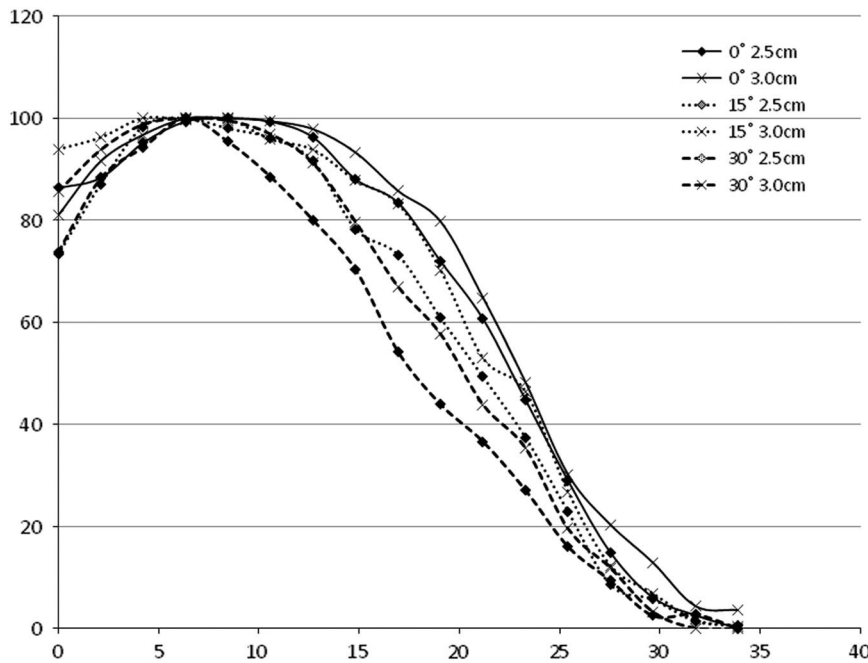


Figure 3. Percentage depth doses graph of 0° (solid line), 15° (dot line) and 30° (dash line) with 2.5 cm (◆) and 3.0 cm (X) applicators.

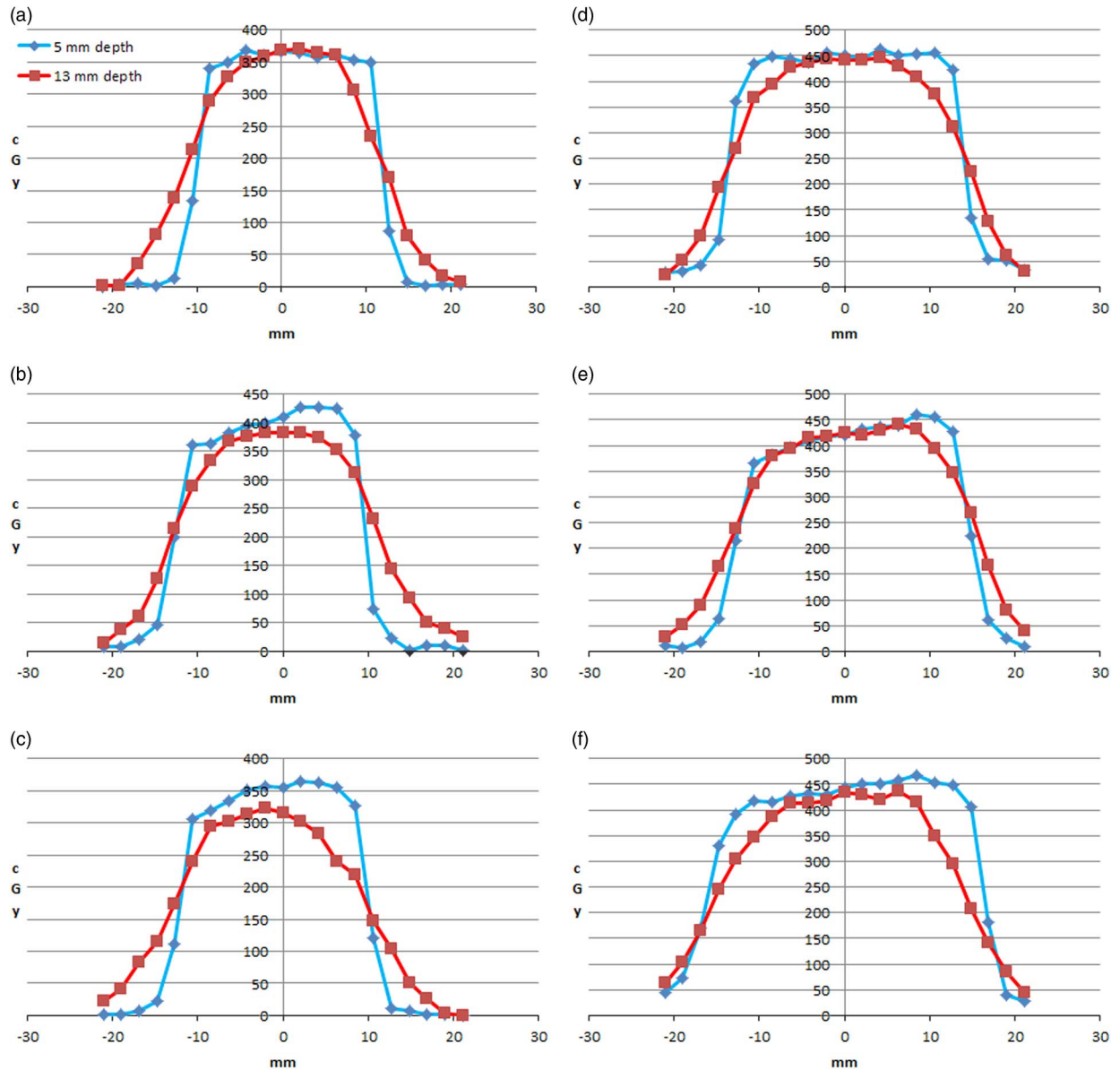


Figure 4. Dose profiles for 2.5 cm applicators [0° (a), 15° (b), 30° (c)] and 3.0 cm applicators [0° (d), 15° (e), 30° (f)]. Measurements were performed for 0.5 cm depth (◆) and 1.3 cm depth (■).

and 1.28 cm. The effective depth for a 6 MeV electron beam is 1.28 cm, and we compared the dose profiles at this depth to the dose profiles at 0.5 cm. Absolute doses at 1.28 cm were greater than those at 0.5 cm in most cases, but not all. We consider these results to be due to differences in the applicator slopes: the dose profiles for sloped applicators show tilted shapes, while the dose profiles for non-sloped applicators show flat shapes. Figure 4 shows the dose profiles for each angle and depth.

### Secondary cancer risk

The secondary cancer risks for the thyroid and both eyes were calculated based on secondary doses at OAR, which were measured ten times during IORT using RPLGDs. Of the ten measurements, one measurement was an outlier from average value, so we calculated the secondary cancer risk from the other nine measurements. Standard deviation was decreased by excluding this outlier. The calculation assumes initiation of treatment at the age of 30. Secondary cancer risks

**Table 1.** Calculation results of each item when patients receive treatment at the age of 30 years and live until 50 years

Site	<i>a</i>	<i>e</i>	OED	$\frac{S(a)}{S(e)}$ (F)	$\frac{S(a)}{S(e)}$ (M)	LAR (F)	LAR (M)
Thyroid	50	30	0.09576	0.95	0.94	48	6
R-eye	50	30	0.41885	0.95	0.94	3	4
L-eye	50	30	0.41896	0.95	0.94	3	4

Abbreviations: OED, organ effective dose; LAR, lifetime attributable risk.

**Table 2.** Calculation results of each item when patients receive treatment at the age of 30 years and live until 80 years

Site	<i>a</i>	<i>e</i>	OED	$\frac{S(a)}{S(e)}$ (F)	$\frac{S(a)}{S(e)}$ (M)	LAR (F)	LAR (M)
Thyroid	80	30	0.09576	0.48	0.35	122	22
R-eye	80	30	0.41885	0.48	0.35	13	18
L-eye	80	30	0.41896	0.48	0.35	13	18

Abbreviations: OED, organ effective dose; LAR, lifetime attributable risk.

were calculated for hypothetical cases wherein patients lived until the ages of 50 and 80. As shown in Table 1, if 100,000 female patients receive tongue cancer treatment at 30 years and live until 50 years, 48 will develop thyroid cancer, three will develop cancer of the right eyes, and three will develop cancer of the left eyes. In the case of 100,000 male patients, six will develop thyroid cancer, four will develop cancer of the right eyes and four will develop cancer of the left eyes. If 100,000 female and 100,000 male patients receive IORT to the tongue at age 30 years and live until 80 years, thyroid cancer would develop in 122 women and 22 men, ocular melanoma or retinoblastoma at right eye in 13 women and 18 men, and ocular melanoma or retinoblastoma at left eye in 13 women and 18 men. Tables 1 and 2 present these data more fully.

**DISCUSSION**

We analysed 6 MeV electron-beam dose patterns for IORT for tongue cancer in a water-equivalent phantom. All PDD shapes corresponded well to normal electron PDD patterns for the two diameters and three angles measured. The PDD patterns of the IORT electron beam were similar to those of normal electron beams, but the absolute doses for each acrylic cylinder differed from those for a normal 6 MeV electron

beam. When two acrylic cylinders’ slope angles are the same, the one with the larger diameter will be associated with the greater radiation dose. The maximum doses for the 2.5 and 3 cm diameter cylinders were 394 and 467 cGy, respectively, with a 0° slope. Results for the other cylinder slopes are shown in Figure 3. These results might be due to higher electron attenuation by smaller-diameter acrylic cylinders.<sup>1–3</sup>

Dose distributions were different for each cylinder slope, and absolute doses varied with the measurement depth. Sharp shapes and angular slopes appeared at the shallow 0.5 cm depth, but blunt shapes appeared at the deeper 1.28 cm depth (see Figure 4). The reason why, in some cases, greater doses were present at the 0.5 cm depth than at the 1.28 cm depth is that the acrylic cylinder’s slope influences its original effective depth.

The secondary cancer risk to the thyroid was 9.38 times greater than the risk to the eyes in women and 1.22 times greater in men; the RPLGD on the neck received a greater cumulative dose than those on the eyes (see Tables 1 and 2). Radiation sensitivities of the thyroid and eyes were also included in the secondary cancer risk calculations. Women’s thyroids are more sensitive to radiation than men’s, so the risk of secondary thyroid cancer was higher for women than for men.<sup>24–25</sup> In addition, calculation results for secondary cancer risk from the IORT tongue treatment suggest that <0.1% patients would get secondary cancer at thyroid or both eyes.

**CONCLUSIONS**

In this study, we measured and calculated dose distribution and secondary cancer risk for the IORT with an acrylic cylinder type of electron cone. From the result, we found that all PDD shapes correspond well to normal PDD patterns and the output factor of IORT was changed by cone size. For the secondary cancer risk study, we found that the probability of getting secondary cancer is <0.1%; therefore, the risk for patients who would get IORT tongue cancer treatment will be relatively low.

## Acknowledgements

This work was supported by the General Researcher Program (NRF-2015R1D1A1A09056828), the Nuclear Safety Research Program (Grant No. 1603016) through the Korea Foundation Of Nuclear Safety (KOFONS), granted financial resource from the Nuclear Safety and Security Commission (NSSC), and Radiation Technology Development Program (2013M2A2A4027117) of the Republic of Korea.

## References

1. Abe M, Takahashi M. Intraoperative radiotherapy: the Japanese experience. *Int J Radiat Biol Phys* 1981; 7: 863–868.
2. Nemoto K, Ogawa Y, Matsushita H et al. Intraoperative radiation therapy (IORT) for previously untreated malignant gliomas. *BMC Cancer* 2002; 2: 1.
3. Zachario Z, Sieverts H, Eble MJ, Gfrorer S, Zavitzanakis A. IORT (intraoperative radiotherapy) in neuroblastoma: experience and first results. *Pediatr Surg* 2002; 12: 251–254.
4. Fletcher G H, Shukovsky L J. The interplay of radio-curability and tolerance in the irradiation of human cancers. *J Radiol Electrol* 1975; 56: 383–400.
5. Fletcher G H. Clinical dose response curves of human malignant epithelial tumors. *Br J Radiol* 1973; 46: 1–12.
6. Valentini V, Morganti A G, De Franco A et al. Chemoradiation with or without intraoperative radiation therapy in patients with locally recurrent rectal carcinoma: prognostic factors and long-term outcome. *Cancer* 1999; 86: 2612–2624.
7. Kim H K, Kum O. Development of a parallel electron and photon transport (PMCEPT) code II: absorbed dose computation in homogeneous and heterogeneous media. *J Korean Phys Soc* 2006; 49: 1640–1651.
8. American Association of Physicists in Medicine Task Group 71. A protocol for the determination of absorbed dose from high-energy photon and electron beams. *Med Phys* 1983; 10: 741–771.
9. International Atomic Energy Agency. Absorbed Dose Determination in External Beam Radiotherapy: An International Code of Practice for Dosimetry Based on Standards of Absorbed Dose to Water. Technical Series No. 398. Vienna: IAEA 2000.
10. Chung J B, Lee J W, Suh T S et al. Dosimetric characteristics of standard and micro MOSFET dosimeters as in-vivo dosimeter for clinical electron beam. *J Korean Phys Soc* 2009; 55: 2566–2570.
11. Anderson L L, Harington P J, St Germain J. Physics of intraoperative high-dose-rate brachytherapy. In: Gunderson L L, Willet C G, Harrison L B, Calvo F A (eds). *Intraoperative Irradiation: Techniques and Results*. Totowa, NJ: Humana Press, 2000: 87–104.
12. Biggs P J, Epp E R, Ling C C, Novack D H, Michaels H B. Dosimetry, field shaping and other considerations for intraoperative electron therapy. *Int J Radiat Biol Phys* 1981; 7: 875–884.
13. Chu S S, Kim G E, Loh J L. Design and dose distribution of docking applicator for an intraoperative radiation therapy. *Korean Soc Ther Radiol* 1991; 9 (1): 123–130.
14. American Association of Physicists in Medicine Task Group 72. Intraoperative radiation therapy using mobile electron linear accelerators. *Med Phys* 2006; 33: 1476–1509.
15. Piriz G H, Lozano E, Banguero Y et al. Implementation of intraoperative radiotherapy in a linear accelerator VARIAN 21EX. *Rev Bras Fis Med* 2001; 5: 31–34.
16. Piesch E, Burgkhardt B, Vilgis M. Photoluminescence dosimetry: process and present state of art. *Radiat Prot Dosim* 1990; 33: 215–225.
17. Asahi Techno Glass Corporation. RPL Glass Dosimeter/ Small Element System: Dose Ace. Tokyo: Asahi Techno Glass, 2000.
18. Hus S M, Yeh S H, Lin M S, Chen W L. Comparison on characteristics of radiophotoluminescent glass dosimeters and thermoluminescent dosimeters. *Radiat Prot Dosim* 2006; 119: 327–331.
19. Araki F, Moribe N, Shimonobou T, Yamashita Y. Dosimetric properties of radiophotoluminescent glass rod detector in high-energy photon beams from a linear accelerator and cyber-knife. *Med Phys* 2004; 31: 1980–1986.
20. International Commission on Radiation Units and Measurements. Prescribing, recording, and reporting electron beam therapy. *J ICRU* 2004; 4: 5–9.
21. Chung W K, Kim D W. Characteristic study of a radiophotoluminescence radio-photoluminescence glass rod detector for clinical usages: skin and inner body in-vivo verification. *J Korean Phys Soc* 2013; 62: 670–676.
22. Bijan A, Remesh T, Aman A et al. Energy dependence and dose response of Gafchromic EBT2 film over a wide range of photon, electron, and proton beam energies. *Med Phys* 2010; 37: 1942–1965.
23. Bernadette H, Maria M, Oliver J. Technical note: homogeneity of Gafchromic EBT2 film. *Med Phys* 2010; 37: 1753–1825.
24. Schneider U, Kaser-Hotz B. A simple dose-response relationship for modeling secondary cancer incidence after radiotherapy. *Med Phys* 2005; 15: 31–37.
25. Schneider U, Zwahlen D, Ross D, Kaser-Hotz B. Estimation of radiation-induced cancer from three-dimensional dose distributions: concept of organ equivalent dose. *Int J Radiat Biol Phys* 2005; 61: 1510–1515.